WPS1-PR(18) 21345

G Plunk et al.

Stellarators resist turbulent transport on the electron Larmor scale

Preprint of Paper to be submitted for publication in
Physical Review Letters

This work has been carried out within the framework of the EUROfusion Consortium and has received funding from the Euratom research and training programme 2014-2018 under grant agreement No 633053. The views and opinions expressed herein do not necessarily reflect those of the European Commission.

Stellarators resist turbulent transport on the electron Larmor scale

G. G. Plunk,* P. Xanthopoulos, G. Weir, and the W7-X Team
Max-Planck-Institut für Plasmaphysik, Wendelsteinstr. 1, 17491 Greifswald, Germany

Electron temperature gradient (ETG) driven turbulence, despite its ultra-fine scale, is thought to drive significant thermal losses in magnetic fusion devices – but what role does it play in stellarators? The first numerical simulations of ETG turbulence for the Wendelstein 7-X stellarator, together with heat pulse analysis from its initial experimental operation phase, suggest that the associated transport should be negligible compared to other channels. The effect, we argue, originates essentially from the geometric constraint of multiple field periods, a generic feature of stellarators.

Nominally, the thermal transport due to turbulence driven by the electron temperature gradient, arising on the electron Larmor scale (*i.e.* "electron-scale" or ETG turbulence), should be weaker by a factor of the square root of the ion-to-electron mass ratio, *e.g.* $\sqrt{m_i/m_e} \sim 40$ for hydrogen, as compared to turbulence on the ion Larmor scale ("ion-scale turbulence", *e.g.* ion-temperature-gradient-driven); this is due to the disparity in the scales involved. In actuality, however, electron-scale turbulence can exceed this estimate because of the operation of different "nonlinear saturation" physics, which can lead to the formation of finger-like turbulent structures, called "streamers", that convect heat away from the centre of the plasma [1, 2]. Indeed, in tokamak experiments, it has been confirmed that this turbulence can cause a significant fraction of thermal losses, limiting the overall performance of the device [3]. A pressing question is whether Wendelstein 7-X (W7-X), the world's largest fusion facility of the stellarator type, which completed already its initial operation phase, is confronted with this threat as well. In this Letter, we compare the electron heat transport from a series of numerical simulations of electron-scale turbulence, based on the given experimental profiles, against the experimental levels inferred from heat pulse analysis [4] for a representative discharge of the first W7-X operation phase. The radial variation of the latter, we find, is inconsistent with the physics of the ETG mode, and in fact anti-correlates with the simulated levels, leading to the conclusion that ETG turbulence cannot account for the measured transport. Next, we address a complementary scenario, in which the ions are thermally coupled to electrons over the entire radius, as in high density plasmas (so-called high-performance discharges) that are more relevant for the production of fusion energy. In this scenario too, our theoretical findings suggest that electron-scale turbulence does not contribute significantly to transport, being in this case greatly exceeded by ion transport levels. We proceeded to analyze our numerical results on fundamental grounds, to determine their physical meaning and generality. We arrive at the conclusion that electron-scale turbulence in W7-X may be classified by comparison to two limiting cases, characterized by different power laws of the fluctuation spectrum. One limit is the ideal three-dimensional ("slab") regime, exhibiting a known $-7/3$ power law [5], and the other limit is a two-dimensional ("toroidal") regime, giving rise to a $-11/3$ power law, which we explain theoretically in terms of a two-dimensional forward cascade of electrostatic energy. Interestingly, both these regimes appear also in the context of ion-scale turbulence [6], with the important distinction that, for the case of electron-scale turbulence, zonal flows play no measurable role in determining which regime is accessible. Instead, it is simple linear physics that regulates the regime, with the transition between the linear mode branches being essentially controlled by magnetic geometry. However, we note that the absence of toroidal symmetry is *not* an essential factor, as the behavior of electron-scale turbulence in W7-X resembles that in tokamaks with negative or small positive magnetic shear, e.g., at the edge region of the device.

Numerical setup. The simulations were performed employing the massively parallel code GENE [7], which solves the coupled system of nonlinear gyrokinetic equations. According to this well-established theory [8], the fully kinetic description of the magnetized plasma is reduced by one dimension, owing to the fast gyration of particles about the magnetic field lines. We numerically parameterize the five dimensional space $(x, y, z, v_\parallel, \mu)$ (x, y, z are the radial, binormal and parallel spatial coordinates, $v_\parallel$ is the velocity parallel to the magnetic field and μ the magnetic moment) using a computational box with $120 \times 120 \times 120 \times 40 \times 20$ grid points. The spatial domain sizes are $L_x = L_y = 6\rho_s$, and $L_z = 2\pi a$, where ρ_s is the ion Larmor radius, and a is a reference minor radius. Morevover, the ETG fluctuations are assumed electrostatic (with no magnetic field component). For all simulations, only one species is treated kinetically, while the other is assumed to satisfy a Boltzmann distribution.

To facilitate the comparison with analytical theory, the gyrokinetic simulations were performed using a "flux-tube" [9] spatial domain. The magnetic equilibria were generated with the VMEC code [10]. For W7-X, we selected the vacuum "standard" configuration (all non-planar coils carry the same amount of current), and for the tokamak we consider circular magnetic surfaces, either with radially increasing safety factor, which provides the "positive-shear" tokamak ($\hat{s} = 0.5$ on the selected

magnetic surface) or with radially decreasing safety factor, providing the "negative-shear" tokamak ($\hat{s} = -0.5$). Both tokamak configurations have an aspect ratio of 3.5.

Results. We can compare our simulation results with findings from Program XP20160309.10 of the first experimental campaign (OP1.1) of W7-X. As inferred by the temperature profiles, shown in Fig. 1, the electrons in the core region are much hotter than the ions, due to the thermal decoupling of the species that occurs at low density, although the temperatures become roughly equal toward the edge. These conditions are, in principle, sufficient for the excitation of ETG turbulence over the majority of the plasma volume, since the electron temperature gradient exceeds the density gradient (and even the ion temperature gradient) at most radial positions. However, the electron thermal transport, here represented by the effective electron thermal diffusivity $\chi_e^{\rm eff}$ (see middle column in Fig. 1), appears anti-correlated with the estimates from gyrokinetic simulations. Instead, the electron transport is clearly correlated with the density gradient, implicating density-gradient-driven microinstabilities (*e.g.* trapped-particle instabilities). We note that the initial radial increase of the simulated diffusivity $\chi_e^{\rm gk}$, is consistent with the destabilization of the ETG mode with increasing values of the temperature gradient and temperature ratio (T_i/T_e), while the subsequent reduction of $\chi_e^{\rm gk}$ in the outer region can be attributed to mode stabilization by the density gradient. The radial dependence of experimentally measured ion diffusivity, on the other hand, is strongly indicative of ITG turbulence: The diffusivity $\chi_i^{\rm eff}$ (see right column in Fig. 1) grows in the first half of the plasma radius due to the increasing temperature gradient, and subsequently drops in the outer region, due to the strong density gradient.

We now turn our attention the scenario of a high density discharges, where ions and electrons are thermally coupled. Such plasmas are an attractive option for fusion power, and will be systematically explored in subsequent W7-X experimental campaigns. In Fig. 2, we compare the ion thermal flux Q_i from an ion-scale turbulence simulation in W7-X, to the electron heat flux Q_e from an electron-scale turbulence simulation, setting the electron and ion temperature gradients to the same value. The striking observation here is that the ion thermal flux exceeds the electron thermal flux by about an order of magnitude. Although the exact value of the ratio of fluxes is dependent on parameters, our simulation results generally imply that the electron contribution should only be a small part of the total thermal flux when the electron and ion profiles are strongly coupled. To gain insight into the significance of the above findings, let us compare the W7-X results with simulations of a standard, positive-shear tokamak core configuration. It is well known that such simulations, using the adiabatic ion approximation, typically do not even reach saturation [11, 12], and can produce electron flux levels exceeding the ion flux, even

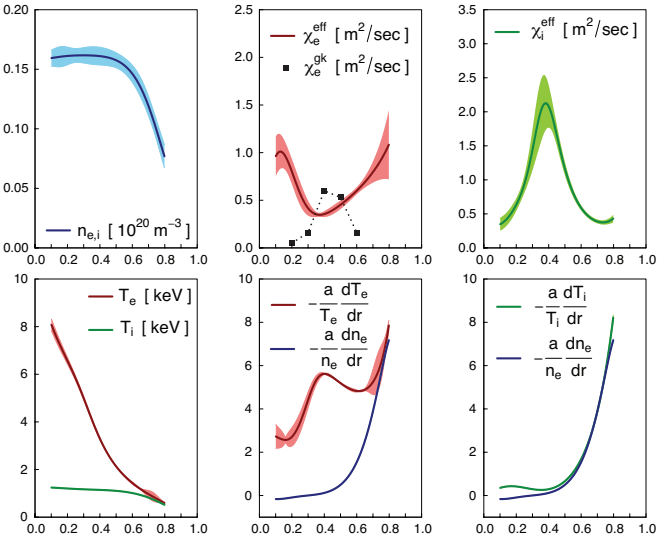

FIG. 1: Density and ion and electron temperature profiles (left column) with associated gradients (middle and right columns, bottom) for a W7-X limiter discharge. The plasma was fueled by hydrogen gas, and was ECRH-heated by 3 Gyrotrons with total power of 2 MW. Electron heat diffusivities (middle column, top) from heat pulse propagation analysis using ECE diagnostics ($\chi_e^{\rm eff}$) and gyrokinetic simulations ($\chi_e^{\rm gk}$) are presented for comparison. The ion heat diffusivity (right column, top) was extracted from XICS diagnostics.

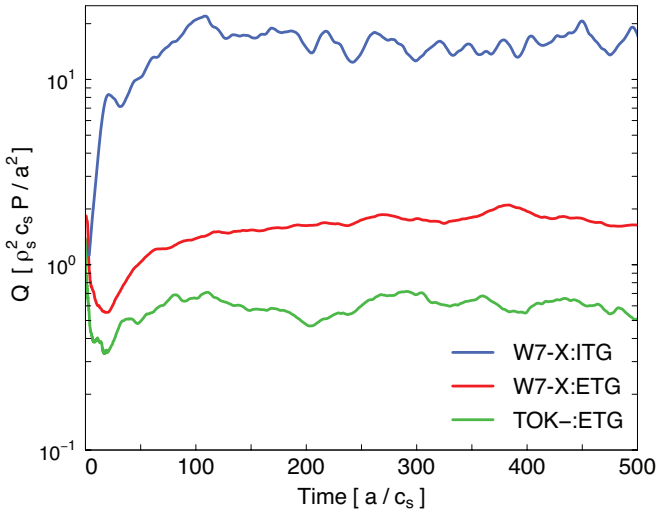

FIG. 2: Comparison of heat fluxes from GENE simulations; ρ_s is the ion gyro-radius, c_s the sound speed, P the pressure and a the minor radius. The heat flux caused by electron-scale turbulence for the W7-X stellarator (W7-X:ETG) and the negative-shear tokamak (TOK-:ETG) are compared to the heat flux caused by equally-driven ion-scale turbulence (W7-X:ITG), *i.e.* $a/L_{T_{i,e}} = 3$.

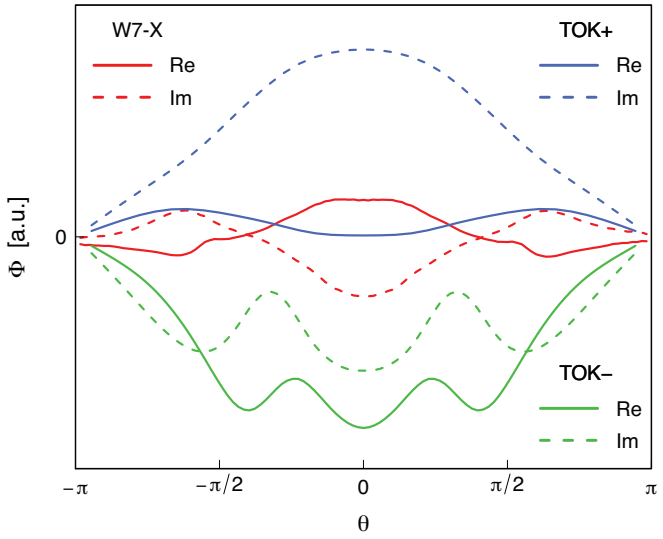

FIG. 3: Mode variation along the magnetic field line for linear modes in the positive-shear tokamak (TOK+), the negative-shear tokamak (TOK-) and the stellarator (W7-X). For each case, the wavenumber chosen corresponds to the peak of the nonlinear heat flux spectrum.

with the inclusion of kinetic ions [7]. The tremendous enhancement of electron fluxes in the positive-shear regime means that electron-scale turbulence must be considered as a key contributor to heat transport at least in the central part of a tokamak plasma. This notion has spurred the tokamak community to turn to "multi-scale" numerical simulations, spanning both electron and ion scales, costing on the order of a million cpu hours each [13]. The insignificant fraction of heat flux carried by electron-scale turbulence in the stellarator, on the other hand, as suggested by our findings, implies that much more affordable single-scale simulations might suffice. A significant fact, evidenced by Fig. 2, is that the negative-shear tokamak, like W7-X, also exhibits a low level of heat flux, ruling out lack of toroidal symmetry as the only possible cause. The suppression caused by magnetic shear has been explained in terms of the different nonlinear saturation mechanisms controlling the amplitude of the two branches of the linear mode [1]. As demonstrated in Fig. 3, the negative-shear tokamak, similar to the stellarator, exhibits oscillatory linear mode structure associated with the slab branch, which saturates by an instability driven by gradient in parallel electron flow [14]. In the positive-shear (standard) tokamak, on the other hand, a strongly toroidal linear mode is excited, subject to a much weaker, two-dimensional instability, causing it to grow to much higher amplitudes. Turning to the nonlinear picture, the toroidal mode excited in the tokamak gives rise to radially elongated streamers, as shown in Fig. 4. Such structures, however, tend to break up in the negative-shear tokamak, and also in the stellarator.

Although the qualitative features of linear eigenfunctions (see Fig. 3) and density fluctuations (see Fig. 4) are physically intuitive signatures of the turbulence regime, we find that the fluctuation spectrum $E(k_y) = \sum_{k_x} |\hat{\phi}|^2/2$ can be used as a quantitative measure. In theory, two possible extremes exist: (i) the fully 3D (slab) limit $E \sim k_y^{-7/3}$, which has been observed in ion-scale turbulence [5], and (ii) the 2D (toroidal) limit $E \sim k_y^{-11/3}$, for which we now outline a new cascade model based on the two-dimensional fluid limit of gyrokinetics. Neglecting linear terms, the following equation may be obtained in the limit $k_\perp^2 \rho_e^2 \ll 1$ (the detailed derivation will be published later):

$$\partial_t \varphi + \hat{\mathbf{z}} \times \boldsymbol{\nabla}\varphi \cdot \boldsymbol{\nabla}(-\nabla^2\varphi - \nabla^2\chi) + \hat{\mathbf{z}} \times \boldsymbol{\nabla}\chi \cdot \boldsymbol{\nabla}(-\nabla^2\varphi) = 0, \quad (1)$$

where χ is the perturbed normalized perpendicular electron pressure, and φ the normalized electrostatic potential. The electrostatic energy $E = \int dxdy\, \varphi^2/2$ is conserved under nonlinear interactions for this system, but, unlike the closely related Hasegawa-Mima equation (valid only for cold ions), this energy can cascade in the forward sense (to smaller scales), due to the absence of an additional quadratic invariant analogous to enstrophy. From this point, it is straightforward to demonstrate that such a cascade leads to the spectrum $E(k_y) \sim k_y^{-11/3}$. This power law seems to be a good match for the positive-shear tokamak, as shown in Fig. 5, while both the negative-shear tokamak and W7-X appear close to the pure slab limit.

Geometric control of mode branch. Since the nonlinear regime is fundamentally linked to linear physics, we examine the linear theory of the electron temperature gradient (ETG) mode, in order to determine a condition regulating the transition between the two branches of the mode. This condition, we find, is of purely geometric nature, *i.e.* independent of plasma conditions, like the temperature gradient. We consider an equation for $\hat{\phi}$, the amplitude of the ETG mode, formally valid in the non-resonant limit at low trapped particle fraction. In a normalized form, this equation reads (see *e.g.* Eqn. (15) of [15]):

$$\left[\hat{\omega}^3 - b_* g(\vartheta)\hat{\omega}^2 + f(\vartheta)\hat{\omega} + \frac{R_c}{4b_* L_\parallel}\frac{d^2}{d\vartheta^2}\right]\hat{\phi}(\vartheta) = 0. \quad (2)$$

Note that we neglect the density gradient, which stabilizes both branches. In equation (2), the frequency is normalized by the nominal growth rate of the toroidal ETG mode, $\hat{\omega} = \omega\sqrt{R_c L_{Te}}/(v_{\mathrm{th,e}} k_y \rho_e)$ (k_y is the binormal wavenumber; ρ_e is the electron Larmor radius; $v_{\mathrm{th,e}}$ is the electron thermal velocity; R_c is the local radius of magnetic curvature, here assumed comparable to the device major radius; L_{Te} is the electron temperature

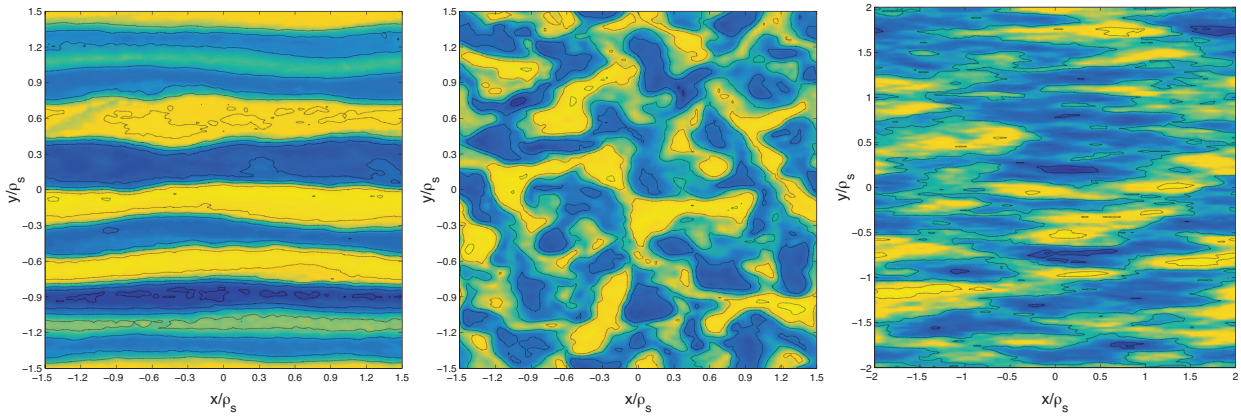

(a) TOK+ configuration. (b) TOK- configuration. (c) W7-X stellarator.

FIG. 4: Density fluctuations from GENE simulations of electron-scale turbulence plotted in the plane perpendicular to the magnetic field. The positive-shear tokamak (TOK+), the negative- shear tokamak (TOK-) and the stellarator Wendelstein-7X are compared. Here, x denotes the radial coordinate and y the binormal coordinate.

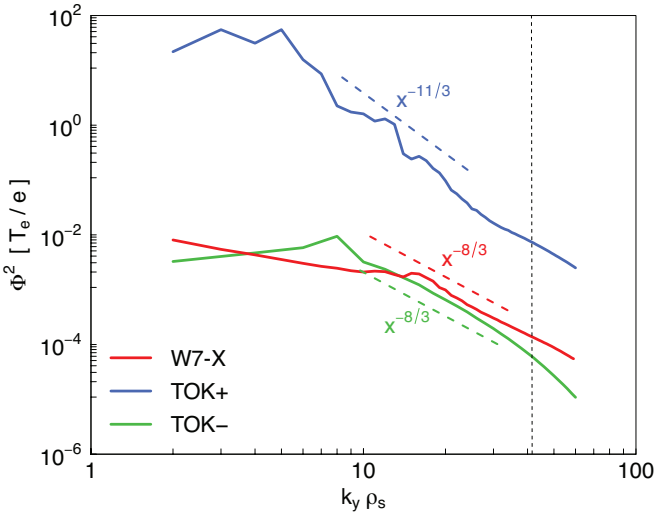

FIG. 5: Fluctuation spectra for electron-scale turbulence compared against power laws. The negative-shear tokamak (TOK-) and W7-X configurations are compared with $k_y^{-8/3}$, which is slightly steeper than the slab limit $k_y^{-7/3}$, while the positive-shear tokamak (TOK+) matches the theoretical law $k_y^{-11/3}$, corresponding to two-dimensional (toroidal) turbulence. Note that these power laws apply for wavenumbers larger than the injection scale and less than $k_y\rho_e = 1$ (vertical line).

gradient length), and therefore $\hat{\omega} \sim 1$ when the mode is toroidal. The equation is differential in the angular coordinate $\vartheta = \pi l/L_\parallel$, *i.e.* the arc-length along the field line l divided by the connection length $L_\parallel$. This length is defined such that the dimensionless coefficients f and g vary on the scale $\Delta\vartheta \sim \pi$. Therefore, to be identified as toroidal, a mode must be localized to a region of this scale, implying $d/d\vartheta \gtrsim 1$. The function $g(\vartheta)$ captures the variation along the field line of the finite-Larmor-radius term, while $f(\vartheta)$ plays an analogous role for the toroidal drive; they are defined such that $f(0) = g(0) = 1$. The remaining dimensionless constants are $L_\parallel/R_c$ and $b_* = k_y^2\rho_e^2\sqrt{R_c/L_{Te}}$. Since the finite-Larmor-radius term is stabilizing, we must have $b_* < 1$. Furthermore, observe that the differential term must also be small for the mode to be toroidal, so, since $d/d\vartheta \gtrsim 1$, we find $L_\parallel/R_c > 1/\sqrt{b_*}$, and we therefore conclude $L_\parallel/R_c > 1$ is required for the existence of a toroidal mode. In any toroidal configuration, properties of the magnetic geometry, such as negative magnetic shear, can cause the connection length to be smaller than the usual estimate $L_\parallel \sim qR_c$ (q is the rotational transform), allowing access to the slab regime ($L_\parallel/R_c < 1$). Stellarators benefit from this effect by construction, as they have multiple field periods, a feature which limits the connection length, since geometric quantities like curvature and local magnetic shear vary strongly from one field period to the next [16]. We can estimate a bound on the connection length in a stellarator as $L_\parallel \lesssim R_c/N$, where N is the field period number (*e.g.*, $N = 5$ for W7-X). This implies $L_\parallel/R_c \sim 1/N < 1$. It is due to these reasons that the linear modes in a stellarator exhibit more of a slab-like character than tokamaks, as has been observed before in linear simulations of W7-X, by measuring the relative energetic importance of the parallel and perpendicular resonances [17].

Conclusions. The first gyrokinetic simulations of electron-scale turbulence in the W7-X stellarator suggest that electron-scale turbulence will account for an insignificant fraction of the total heat transport. The theoretical

evidence, complemented by a heat pulse analysis from a typical W7-X limiter discharge, suggests that this conclusion is remarkably insensitive to plasma parameters. Our analysis suggests that ETG suppression can be enjoyed by toroidal configurations with negative or small positive magnetic shear (as in the tokamak edge) and can be further enhanced by the geometric constraint, imposed on stellarator devices, related to multiple toroidal field periods. We have identified this type of mild electron-scale turbulence with a nonlinearly three-dimensional regime, associated with the slab mode, which does not manifest streamers. We have also argued on fundamental theoretical grounds, and based on the cases observed, that electron-scale turbulence in any toroidal configuration should exhibit spectral indices between the theoretical limiting cases of $-7/3$ and $-11/3$, suggesting a common basis for the understanding and comparison of turbulence in disparate magnetic geometries.

Acknowledgements. The authors thank F. Jenko, T. Görler, D. Told, P. Helander and Y. Turkin for physics discussions and technical support, M. Hirsch for the ECE diagnostic, D. Zhang for bolometry diagnostics, N. Pablant for the XICS diagnostic, G. Fuchert for the Thomson scattering diagnostic and T. Stange for ECRH systems modelling. The GENE simulations were performed on the RZG (Germany) and Marconi (Italy) supercomputers.

* gplunk@ipp.mpg.de

[1] F. Jenko and W. Dorland, Phys. Rev. Lett. **89**, 225001 (2002).
[2] F. Jenko and A. Kendl, Phys. Plasmas **9**, 4103 (2002).
[3] D. Told, F. Jenko, P. Xanthopoulos, L. D. Horton, E. Wolfrum, and A. U. Team, Phys. Plasmas **15**, 102306 (2008).
[4] G. Weir, B. J. Faber, K. M. Likin, J. N. Talmadge, D. T. Anderson, and F. S. B. Anderson, Phys. Plasmas **22**, 056107 (2015).
[5] M. Barnes, F. I. Parra, and A. A. Schekochihin, Phys. Rev. Lett. **107**, 115003 (2011).
[6] G. G. Plunk, P. Xanthopoulos, and P. Helander, Phys. Rev. Lett. **118**, 105002 (2017).
[7] F. Jenko, W. Dorland, M. Kotschenreuther, and B. N. Rogers, Phys. Plasmas **7**, 1904 (2000); `www.genecode.org`.
[8] A. J. Brizard and T. S. Hahm, Rev. Mod. Phys. **79**, 421 (2007).
[9] M. A. Beer, S. C. Cowley, and G. W. Hammett, Phys. Plasmas **2**, 2687 (1995).
[10] S. P. Hirschman *et al.*, Phys. Fluids **26**, 3553 (1983).
[11] W. M. Nevins, J. Candy, S. Cowley, T. Dannert, A. Dimits, W. Dorland, C. Estrada-Mila, G. W. Hammett, F. Jenko, M. J. Pueschel, and D. E. Shumaker, Phys. Plasmas **13**, 122306 (2006).
[12] R. E. Waltz, J. Candy, and M. Fahey, Phys. Plasmas **14**, 056116 (2007).
[13] T. Görler, F. Jenko, M. J. Pueschel, and H. Lesch, High Performance Computing in Science and Engineering '09 (2009).
[14] S. C. Cowley, R. M. Kulsrud, and R. Sudan, Phys. Fluids B **3**, 2767 (1991).
[15] G. G. Plunk, P. Helander, P. Xanthopoulos, and J. W. Connor, Physics of Plasmas **21** (2014).
[16] P. Helander, C. D. Beidler, T. M. Bird, M. Drevlak, Y. Feng, R. Hatzky, F. Jenko, R. Kleiber, J. H. E. Proll, Y. Turkin, and P. Xanthopoulos, Plasma Phys. Control. Fusion **54**, 124009 (2012).
[17] V. Kornilov, R. Kleiber, R. Hatzky, L. Villard, and G. Jost, Physics of Plasmas **11**, 3196 (2004).